Effect of Nanoparticles on the Electrohydrodynamic Instabilities of Polymer/Nanoparticle Thin Films

Joonwon Bae, Elizabeth Glogowski, Suresh Gupta, Wei Chen, Todd Emrick, and Thomas P. Russell*

Department of Polymer Science and Engineering, University of Massachusetts, Amherst, Massachusetts 01003

Received December 10, 2007; Revised Manuscript Received January 29, 2008

ABSTRACT: The influence of gold nanoparticles on electrohydrodynamic instabilities in polymer/nanoparticle nanocomposite thin films was studied as a function of nanoparticle concentration, electric field strength, molecular weight, and film geometry. Thin films of polystyrene mixed up to 1 vol % (20 wt %) of gold nanoparticles having polystyrene ligands under an applied electric field showed electrohydrodynamic instability patterns similar to those seen in pure polystyrene. The presence of gold nanoparticles increased the dielectric constant of the films, which led to a systematic reduction in the wavelength of the surface instabilities. Transmission electron microscopy showed that no migration or aggregation of the gold nanoparticles occurred as a result of the applied electric field. This work points to a simple route to reduce the size scale of columnar patterns generated by electrohydrodynamic instabilities.

Introduction

Pattern formation in thin films is of increasing scientific and industrial interest for applications including coating, adhesion, membranes, optical and electronic devices, and sensors. Numerous experimental and theoretical studies have appeared dealing with instabilities and consequent morphologies of thin polymer films induced by external fields.[1–20] These studies focused on phenomena driven dominantly by interfacial energies. Recently, instabilities induced by an external electric field have attracted significant interest, since electric fields can overcome interfacial interactions to produce highly ordered structures. In addition, the influence of electrostatic force on the surface of thin polymer films has been extensively examined.[21–27]

The interaction of an electric field with a dielectric material is well understood, since Swan first investigated the influence of electric fields on the surface of polymers or viscous liquids.[28] When an applied electric field exceeds a critical value, the surface or polymer/air interface becomes unstable, leading to the formation of ordered arrays of columns or pillars on the surface. Driven by differences in the dielectric constants of the two media at the interface, electrohydrodynamic (EHD) instabilities result acting to align the surface of the film parallel to the field direction, thereby minimizing torque at the interface arising from electrostatic forces. The balance between the electrostatic pressure and the Laplace pressure acting on the interface causes the amplification of fluctuations having one characteristic wavelength leading, ultimately, to columns of polymer that span the gap between the upper and lower electrodes used to apply the field. The wavelength of the columns produced is on the order of microns. As the demand for smaller size scale structures increases, alternative methodologies have been used to obtain nanoscopic columnar arrays.[29–32]

One approach is the use of inorganic nanoparticles as fillers for polymer/nanoparticle nanocomposites. Most inorganic nanoparticles have a high dielectric constant, and a uniform dispersion of the nanoparticles within a polymer would increase the average dielectric constant of the nanocomposite. In addition, the nanoparticles can also serve to enhance the mechanical properties and impart unique optical or electronic properties to the compositie. Achieving a uniform dispersion of nanoparticles in the polymer maxtix can be challenging. However, the ligands attached to the nanoparticles can be tailored to interact favorably with the polymer matrix, so that ligand/matrix interactions are much more favorable than ligand/ligand interactions.[33] In this way, homogeneous dispersions of nanoparticles in a polymer matrix can be realized.

Here we present a systematic investigation of electrohydrodynamic instabilities in polystyrene/gold nanoparticle nanocomposites. Results from optical microscopy studies showed a reduction in the wavelength caused by the addition of nanoparticles to the polymer. In addition, no significant migration or aggregation of the nanoparticles occurred as a result of the applied electric field.

Experimental Section

Materials. Polystyrene (PS) with number-average molecular weight of 50K (PDI 1.04) and 160K (PDI 1.05) was purchased from Polymer Source and used without further purification. Polystyrene-functionalized gold nanoparticles (Au(PS)), with an average gold diameter of 4 nm, were prepared by established procedures,[34,35] in a two-step synthesis by reduction of hydrogen tetrachloroaurate with sodium borohydride using polystyrenethiol as ligand. The molecular weight of the PS ligand was 1.1K, and the density of the Au(PS) was 19.3 g/cm^3.

Preparation of Nanocomposite Thin Films. Polystyrene and Au(PS) nanoparticles were dissolved in toluene where the volume fraction of Au(PS) nanoparticles was 0.05, 0.25, 0.5, and 1.0%. The PS/Au(PS) nanocomposite was spin-coated onto silicon wafers that were passivated using a 5% hydrofluoric acid (HF) solution. The thicknesses of the nanocomposite thin films measured by ellipsometry were 250 nm.

Application of Electric Field. A schematic diagram describing the manner in which the electric field was applied is shown in Figure 1.[32] A silicon wafer, coated with nanocomposite thin film, served as one electrode, and a soda-lime glass coated with a thin layer of gold (20 nm) and chromium (5 nm) was the second electrode. A rectangular well was etched in the glass slide by immersion in buffered HF using a poly(methyl methacrylate) mask. The electrode spacing was controlled by varying the etching time: 0.2 μm/min. In this geometry, the dominant gradient in the electric field occurs across the air/nanocomposite film interface, noted by "d" in Figure

* To whom correspondence should be addressed: Fax: 413-545-0082; e-mail: russell@mail.pse.umass.edu.

10.1021/ma702750y CCC: $40.75
Published on Web 03/14/2008

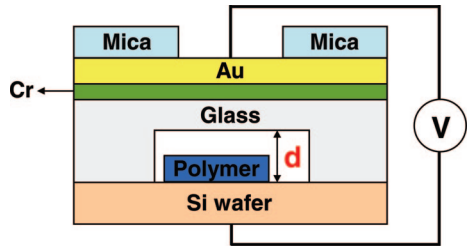

Figure 1. Schematic diagram of experimental setup.

1. A voltage was applied, and the assembly was heated for 4−24 h at 160 °C, well above the glass transition temperature of PS. Then the assembly was quenched to room temperature to freeze the EHD pattern. After each experiment, the upper glass electrode was removed mechanically.

Instrumental Analysis. Film thickness was measured with a Rudolph Research AutoEL-II ellipsometer using a helium−neon laser (λ = 632.8 nm) at a 70° incidence angle. The dielectric constants of PS/Au(PS) were measured with a Novocontro dielectric spectrometer on melt-pressed, 300 μm disk (2.0 cm in diameter) coated with silver adhesive as conductive layers, over a frequency range from 1 MHz to 0.1 Hz at 25 and 160 °C. The EHD instability patterns were observed with an Olympus BX60 optical microscope in reflection mode. Bright field transmission electron microscopy (TEM) studies were performed with a JEOL 100CX TEM operated at an accelerating voltage of 100 kV. To prepare TEM specimens, a thin layer of carbon was evaporated onto the film surface to prevent the diffusion of the epoxy resin into nanocomposite thin film. The thin film was then embedded in an epoxy resin and cured at 60 °C for 18 h. Ultrathin sections (60 nm) were collected at room temperature using a Leica Ultracut Microtome, equipped with a diamond knife.

Results and Discussion

Figure 2a shows a reflection optical microscopic image of a PS/Au(PS) nanocomposite thin film. As can be seen, the film appears to be uniform, flat, and featureless. The EM image (Figure 2b) shows that the Au(PS) nanoparticles were uniformly distributed in the polymer maxtix. The uniform distribution of nanoparticles in the host polymer is a key to ensure uniformity of properties, ranging from mechanical to electrical properties of the nanocomposite. To this end, the Au nanoparticles were functionalized with PS ligands that would be expected to disperse the nanoparticles in a PS matrix. In this case, the enthalphic gain for dispersing the particles is small or zero (due to interactions between the ligand and host polymer), and any entropy loss arising from packing the nanoparticles in the polymer matrix must be minimized. For the studies described here, the nanoparticles were sufficiently small so that configurational entropic losses of the polymer to incorporate the nanoparticles were small, and consequently, a uniform dispersion was achieved (Figure 2b). Experiments were also performed on films annealed at 160 °C, well above the glass transition temperature of the PS, to determine whether a segregation of the nanoparticles to the air surface occurred. Such a nonuniform distribution of nanoparticles would, of course, distort the response of the film to an applied electric field. TEM images of an annealed film are shown in Figure 2c,d. Regardless of the viewing angle, the nanoparticles appear to be uniformly dispersed throughout the film after thermal annealing. The frequency dependence of dielectric constants measured at 25 and 160 °C (temperature range used in this study) were plotted in Figure 2e. As the frequency decreased from 1 MHz to 0.1 Hz, the real part of the dielectric constant of PS 50K/Au(PS) (0.5 vol %) increased slightly (about 5%) at both 25 and 160 °C; on the other hand, the imaginary part shows almost negligible frequency dependence. Because the dielectric constant

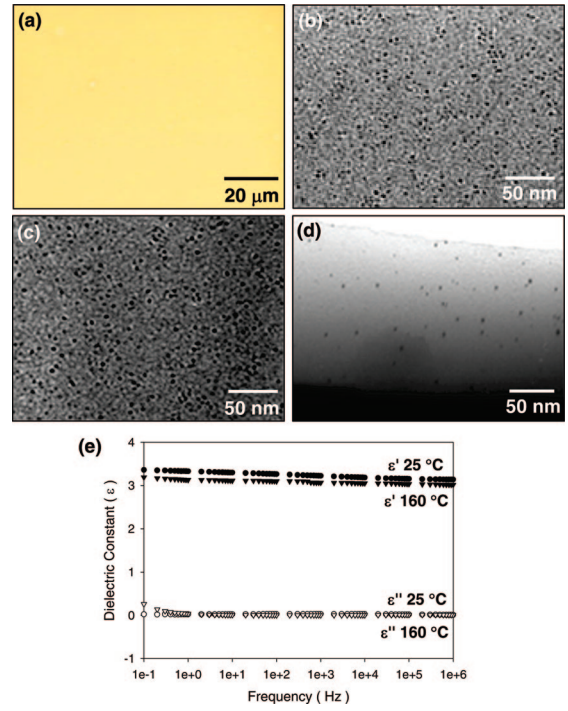

Figure 2. (a) Optical microscope image of the surface of PS 50K/Au(PS) (0.5 vol %) thin film (250 nm); TEM images of PS 50K/Au(PS) (0.5 vol %) thin film (50 nm) (b) before thermal annealing; (c) after thermal annealing at 160 °C for 24 h; (d) microtomed cross section after thermal annealing at 160 °C for 24 h; (e) frequency dependence of dielectric constants measured at 25 and 160 °C.

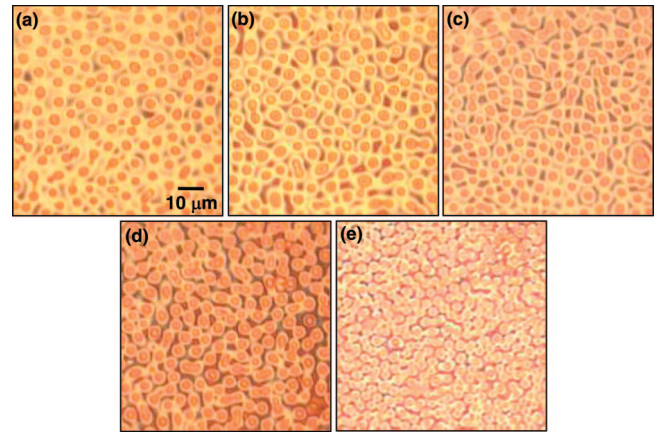

Figure 3. Electrohydrodynamic instability patterns of various PS 50K/Au(PS) thin films (250 nm) as a function of nanoparticle concentration. Electric field of 30 V/μm was applied at 160 °C for 6−8 h. (a) PS 50 K; (b) Au(PS) 0.05 vol %; (c) Au(PS) 0.25 vol %; (d) Au(PS) 0.5 vol %; (e) Au(PS) 1.0 vol %.

of pure PS is ~2.61 at 1 KHz,[36] the obtained dielectric constant value is reasonable. It is confirmed that the introduction of gold nanoparticles into PS matrix led to the increase in dielectric constant of nanocomposite.

The application of a voltage across the electrodes results in a gradient electric field across the surface of the thin film. Capillary waves on the film surface are amplified by the applied electric field, while surface energy acts to suppress the amplification of the fluctuations. The interplay between these gives rise to the growth of fluctuations of one preferred wavelength and results in the formation of columns. Optical microscopy images, shown in Figure 3, are typical electrohydrodynamic instability patterns of various PS/Au(PS) nanocomposite thin films for different nanoparticle concentrations.

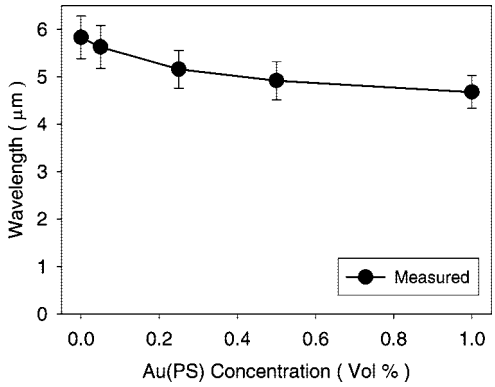

Figure 4. Variation in wavelength of EHD instability pattern of various PS 50K/Au(PS) thin films.

Similar patterns were observed at 30 V/μm for all nanoparticle concentrations. As the nanoparticle concentration increased, the distance between adjacent columns decreased from 5.7 μm for pure PS 50K thin film to 4.8 μm at 1.0 vol % nanoparticles. This is in keeping with recent arguments where the intercolumnar distance of the pattern was predicted to decrease as the dielectric constant of the material increased.[21,37] The reduction in the wavelength with increasing nanoparticle concentration indicates that the nanocomposite thin films behaved like a single-component thin film with the nanoparticles being uniformly dispersed.[38,39] These results show that the use of high dielectric constant nanoparticles as a nanofiller can provide an easy route for the generation of smaller sized surface feature.

When the external electric field is applied, the pressure at the surface of thin liquid film under the applied field is given by

$$P = P_0 + P_{el}(h) + P_{Lap}(h) + P_{dis}(h) \quad (1)$$

where P and P_0 are the pressures in the liquid film and the air, respectively. P_{el} is electrostatic pressure arising from the difference in the dielectric constants between two media

$$P_{el}(h) = -\epsilon_0\epsilon_p(\epsilon_p - 1)E_p \quad (2)$$

where ϵ_0 and ϵ_p are the permittivity in vacuum and the liquid dielectric constant. In addition, E_p is the electric field strength in the liquid layer where h and d are film thickness and air gap in electrode.

$$E_p = \frac{U}{\epsilon_p d - (\epsilon_p - 1)h} \quad (3)$$

The third term P_{Lap} is the Laplace pressure, arising from the interfacial energy contribution due to changes in interfacial area. The disjoining pressure, P_{dis}, arises from the dispersive van der Waals interaction. When the film thickness is greater than 100 nm, the contribution of disjoining pressure is negligible in comparison to the electrostatic pressure. Since the film thicknesses are sufficiently large (250 nm), the disjoining pressure contribution is negligible. According to Schaeffer et al., the characteristic wavelength is given by

$$\lambda_{max} = 2\pi\sqrt{\frac{\gamma U}{\epsilon_0\epsilon_p(\epsilon_p - 1)^2}}\,E_p \quad (4)$$

where U is applied voltage, ϵ_0 and ϵ_p are the permittivity in vacuum and the liquid dielectric constant, γ is surface tension of the polymer, and E_p is electric field strength in the polymer.[37] The wavelength decreases as the dielectric constant of polymer liquid increases. Consistent phenomena were observed in the EHD instability patterns of PS/Au(PS) nanocomposite thin films, as shown in Figure 4. Since the difference in dielectric constants is proportional to the concentration of Au(PS) nanoparticles, the wavelength of columns decreased with increasing Au(PS) concentrations. It is noteworthy that the decrease in the wavelength diminished for nanoparticle concentrations above 0.5 vol %, which is consistent with previous experimental results.[37]

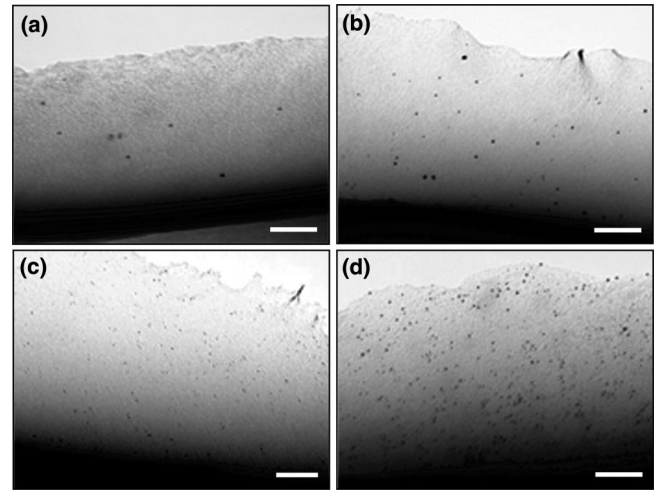

Figure 5. Cross-sectional TEM images of various PS 50K/Au(PS) nanocomposite thin films exposed in the electric field of 30 V/μm for 6−8 h: (a) Au(PS) 0.05 vol %; (b) Au(PS) 0.25 vol %; (c) Au(PS) 0.5 vol %; (d) Au(PS) 1.0 vol %. Scale bar is 50 nm.

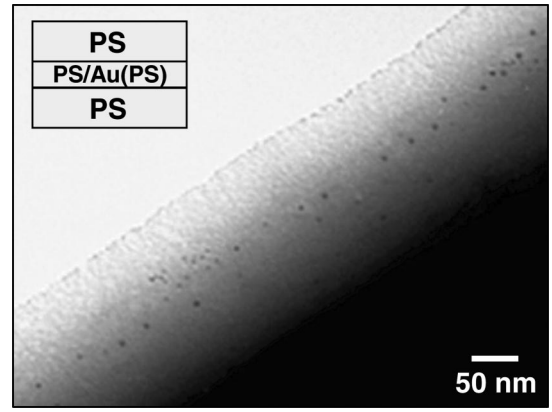

Figure 6. Cross-sectional TEM image of trilayer PS 50K (80 nm)−PS 50K/Au(PS) (1 vol %, 50 nm)−PS 50K (80 nm). The assembly was thermally annealed at 160 °C for 12 h and then exposed to the electric field of 30 V/μm for 8 h.

To visualize the effect of nanoparticles on the EHD instability of thin films, cross-sectional TEM images were taken. The nanocomposite thin films were microtomed perpendicular to the film surface. Figure 5 shows the cross sections of various PS 50K/Au(PS) nanocomposite thin films. In all cases, no migration or segregation of the Au(PS) nanoparticles to the surface occurred during the application of the electric field. Throughout the formation and growth of macroscopic columns, the polymer is continuously drawn into the columns. This flow, of course, produces a movement of nanoparticles. But, judging from the TEM images, the entropy and favorable enthalpic interactions are sufficiently strong to maintain a uniform dispersion. Namely, there is no significant force acting on the individual neutral gold nanoparticles. In addition, the dipole–dipole interaction arising from localized permanent dipole is negligible at these concentrations because the intensity of dipole–dipole interaction is inversely proportional to the sixth power of the distance between Au nanopar-

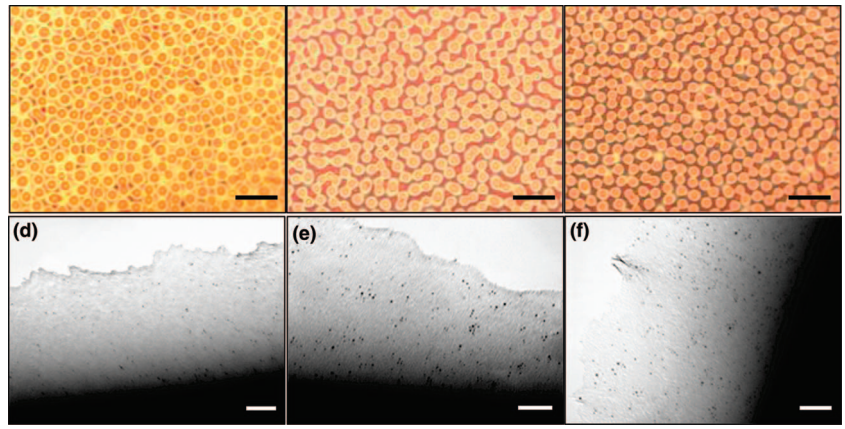

Figure 7. Optical microscope images of EHD stability patterns of PS 160K/Au(PS) (0.5 vol %) nanocomposite thin films exposed in the electric field of (a) 20 V/μm for 24 h, (b) 30 V/μm for 16 h, and (c) 45 V/μm for 12 h. Scale bar is 10 μm. Corresponding cross-sectional TEM images of (d) thin film in a; (e) in b; and (f) in c. Scale bar is 50 nm.

ticles. As shown in Figure 5d, the average distance between neighboring Au nanoparticles is larger than 20 nm.

To see the movement of the nanoparticles during pattern formation, a simple experiment was performed using a three-layer assembly. The PS 50K/Au(PS) (1.0 vol %) thin film with a thickness of 50 nm was sandwiched between two PS 50K thin films (80 nm for each layer). This layered assembly was thermally annealed at 160 °C for 12 h and then exposed to a electric field of 30 V/μm for 8 h. The cross-sectional TEM image in Figure 6 suggests that the nanoparticles are confined in the center region of assembly after EHD instability pattern formation. While there must be flow of PS in the direction of the applied electric field, no migration or segregation of nanoparticles to the surface was observed macroscopically after application of a voltage. We could only observe the short-range diffusion of nanoparticles in the center region of the assembly. This demonstrates that the migration or segregation behavior of Au(PS) nanoparticles under an electric field was not influenced significantly by the flow of PS along the direction of applied electric field during column growth.

It is well-known that the response of a polymer to an electric field depends on the various parameters such as electric field strength, molecular weight, dielectric constant, and viscosity. Herein, we have further investigated the effect of nanoparticles on the EHD instability by controlling two important parameters: the strength of the electric field and the molecular weight of PS matrix. As with the 50K PS, a reduction in wavelength was also observed in EHD instability of the PS 160K/Au(PS) nanocomposite system. The optical miscoscopy images of instabilities observed in PS 160K/Au(PS) (0.5 vol %) thin films exposed to various electric field are presented in Figure 7 a−c. It is clear that the dependence of wavelength on the intensity of applied electric is much less remarkable than the nanoparticle effect. The wavelength changed slightly from 3.7 to 3.4 μm with increasing electric field intensity from 20 to 45 V/μm. Figure 7 d−f shows cross-sectional TEM images of several PS 160K/Au(PS) (0.5 vol %) nanocomposite thin films after applying electric fields of different strengths. It was reported that the electric field exposure time required to obtain columnar arrays on the surface of homopolymer was inversely proportional to the electric field strength and proportional to the molecular weight of polymer.[24] So even longer exposure times (16−24 h) were necessary to generate EHD instability patterns. TEM images in Figure 7 indicate that no migration or segregation of the nanoparticles occurred during pattern formation. As the molecular weight of PS increased from 50K to 160K, the favorable interaction between PS matrix and Au(PS) nanoparticle surface did not change considerably. Owing to the larger radius of gyration of 160K PS (12.7 nm), the entropic penalty associated with the size of nanoparticles decreased. Therefore, the Au(PS) nanoparticles are distributed uniformly in the 160K PS matrix. While a smaller intercolumn wavelength was obtained at high electric field strengths, there is no clear effect on the nanoparticle distribution in the PS matrix.

Conclusions

The electrohydrodynamic instability of the polymer/nanoparticle system was systematically investigated as a function of nanoparticle concentration, molecular weight of matrix polymer, and electric field strength. The incorporation of nanoparticles with high dielectric constant increased the dielectric constant of nanocomposite thin film materials, leading to a systematic reduction in the length scale of the instability pattern. No migration or segregation resulted from the applied external electric field, indicating that the polymer/nanoparticle nanocomposites responded to the electric field without altering the structures and properties. This study provides a simple route for generation of smaller sized structures by EHD instability and demonstrates experimentally the use of EHD instability on nanocomposite systems.

Acknowledgment. This work was supported by the Department of Energy, Office of Basic Energy Sciences, and also supported in part by the Korea Research Foundation Grant funded by the Korean Government (KRF-2005-214-D00272), and the NIRT-CBET (0609107).

References and Notes

(1) Vrij, A. *Discuss Faraday Soc.* **1966**, *42*, 23.
(2) Williams, M. B.; Davis, S. H. *J. Colloid Interface Sci.* **1982**, *90*, 220.
(3) Sharma, A.; Ruckenstein, E. *Langmuir* **1986**, *2*, 480.
(4) Brochard-Wyart, F.; Daillant, J. *Can. J. Phys.* **1991**, *68*, 1984.
(5) Reiter, G. *Phys. Rev. Lett.* **1992**, *68*, 75.
(6) Yerushalmi-Rosen, R.; Klein, J.; Fetters, L. *Science* **1994**, *263*, 793.
(7) Onuki, A. *Physica A* **1995**, *217*, 38.
(8) Sharma, A.; Khanna, R. *Phys. Rev. Lett.* **1998**, *81*, 3463.
(9) Boltau, M.; Walheim, S.; Mlynek, J.; Krausch, G.; Steiner, U. *Nature (London)* **1998**, *391*, 877.
(10) Sferrazza, M.; Heppenstall-Butler, M.; Cubitt, R.; Bucknall, D.; Webster, J.; Jones, R. A. *Phys. Rev. Lett.* **1998**, *81*, 5173.
(11) Xie, R.; Karim, A.; Douglas, J. F.; Han, C. C.; Weiss, R. A. *Phys. Rev. Lett.* **1998**, *81*, 1251.
(12) Chou, S. Y.; Zhuang, L.; Guo, L. *Appl. Phys. Lett.* **1999**, *75*, 1004.
(13) Gau, H.; Herminghaus, S.; Lenz, P.; Lipowsky, R. *Science* **1999**, *283*, 46.
(14) Oron, A. *Phys. Rev. Lett.* **2000**, *85*, 2108.
(15) Reiter, G.; Khanna, R.; Sharma, A. *Phys. Rev. Lett.* **2000**, *85*, 1432.
(16) Thiele, U.; Velarde, M. G.; Neuffer, K. *Phys. Rev. Lett.* **2001**, *87*, 016104.

(17) Warner, M. R. E.; Craster, R. V.; Matar, O. K. *J. Colloid Interface Sci.* **2003**, *268*, 448.
(18) Pease, L. F., III; Russel, W. B. *J. Chem. Phys.* **2003**, *118*, 2790.
(19) Pease, L. F., III; Russell, W. B. *Langmuir* **2004**, *20*, 795.
(20) Sharnkar, V.; Sharma, A. *J. Colloid Interface Sci.* **2004**, *274*, 294.
(21) Schaeffer, E.; Thurn-Albrechet, T.; Russell, T. P.; Steiner, U. *Nature (London)* **2000**, *403*, 874.
(22) Morariu, M. D.; Voivu, N. E.; Schaeffer, E.; Lin, Z.; Russell, T. P. *Nat. Mater.* **2003**, *2*, 48.
(23) Lin, Z.; Kerle, T.; Russell, T. P. *Macromolecules* **2002**, *35*, 6255.
(24) Lin, Z.; Kerle, T.; Russell, T. P.; Schaeffer, E.; Steiner, U. *Macromolecules* **2002**, *35*, 3971.
(25) Xu, T.; Hawker, C. J.; Russell, T. P. *Macromolecules* **2003**, *36*, 6178.
(26) Xiang, H.; Lin, Y.; Russell, T. P. *Macromolecules* **2004**, *37*, 5358.
(27) Leach, K. A.; Lin, Z.; Russell, T. P. *Macromolecules* **2005**, *38*, 4868.
(28) Swan, J. W. *Proc. R. Soc. London* **1897**, *62*, 38.
(29) Wu, N.; Pease, L. F., III; Russel, W. B. *Adv. Funct. Mater.* **2006**, *16*, 1992.
(30) Harkema, S.; Steiner, U. *Adv. Funct. Mater.* **2005**, *15*, 2016.
(31) Verma, R.; Sharma, A.; Kargupta, K.; Bhaumik, J. *Langmuir* **2005**, *21*, 3710.
(32) Leach, K. A.; Gupta, S.; Dickey, M. D.; Wilson, C. G.; Russell, T. P. *Chaos* **2005**, *15*, 047506.
(33) Balazs, A. C.; Emrick, T.; Russell, T. P. *Science* **2006**, *5802*, 1107.
(34) Chiu, J. J.; Kim, B. J.; Kramer, E. J.; Pine, D. J. *J. Am. Chem. Soc.* **2005**, *127*, 5036.
(35) Brust, M.; Walker, M.; Betell, D.; Schiffrin, D. J.; Whyman, R. *J. Chem. Soc., Chem. Commun.* **1994**, *801*000.
(36) *Polymer Data Handbook*; Mark, J., Ed.; Oxford University Press: New York, 1999; p 830.
(37) Lin, Z.; Kerle, T.; Baker, S. M.; Hoagland, D. A.; Schaeffer, E.; Steiner, U.; Russell, T. P. *J. Chem. Phys.* **2001**, *114*, 2377.
(38) Smith, K. A.; Tyagi, S.; Balazs, A. C. *Macromolecules* **2005**, *38*, 10138.
(39) Lee, J. Y.; Balazs, A. C.; Thompson, R. B.; Hill, R. M. *Macromolecules* **2004**, *37*, 3536.

MA702750Y